Mechanical Properties of Waxy Maize Starch Nanocrystal Reinforced Natural Rubber

Hélène Angellier,[†] Sonia Molina-Boisseau,[†] and Alain Dufresne*[,‡]

Centre de Recherches sur les Macromolécules Végétales (CERMAV-CNRS), Université Joseph Fourier, BP 53, 38041 Grenoble Cedex 9, France, and Ecole Française de Papeterie et des Industries Graphiques de Grenoble (EFPG-INPG), BP 65, 38402 St Martin d'Hères Cedex, France

Received June 13, 2005; Revised Manuscript Received August 19, 2005

ABSTRACT: In a previous work [*Macromolecules* **2005**, *38*, 3783], nanocomposite materials obtained from a latex of natural rubber (NR) as matrix and an aqueous suspension of waxy maize starch nanocrystals as filler were processed and characterized in terms of morphology, structural, and barrier properties. The aim of the present work was to study the mechanical properties of these materials in both the linear and nonlinear range. It was shown that up to a content of 20 wt % this new filler presents the advantage to reinforce NR without decreasing significantly the elongation at break of the material. The relaxed modulus at room temperature of nanocomposite films containing 20 wt % of filler is 75 times higher than the one of the unfilled matrix. Particle−particle interactions play a crucial role in the properties of starch nanocrystals filled NR. The effect of moisture content and surface chemical modification of the starch nanocrystals on the reinforcing properties was also investigated.

Introduction

Soft rubbery materials display a characteristic elastic behavior and are used for many important engineering products. Most are reinforced with fillers, notably carbon black, silica, or calcium-based powders, to achieve enhanced mechanical performances. Generally, the increase in modulus is achieved at the expense of strength and elongation at break. There are some exceptions, particularly carbon black, which induces an increase in both strength and modulus, but also a significant decrease in elongation at break. The reinforcing effect increases with the amount of filler added and also with reduction in particle size.[1] Recently, a variety of clays such as montmorillonite and organoclays[2−9] have been used to obtain unusual nanocomposites by exploiting the ability of the clay silicate layers to disperse into polymer matrices.

As recently shown,[10,11] aqueous suspensions of nanometer size crystalline nanoplatelets with a well-defined morphology can be obtained from the sulfuric acid hydrolysis of amylopectin-rich "waxy" maize native starch granules. These starch nanocrystals displayed interesting reinforcing properties when they are dispersed in poly(styrene-*co*-butyl acrylate).[12] In this context, waxy maize starch nanocrystals have been considered as potential filler for natural rubber (NR), which is one of the most important elastomers, widely used in industrial and technological areas. This nanoconcept is highly relevant for rubber compounds since their application requires filler reinforcement. In a previous article,[13] nanocomposite materials were obtained using latex of NR as the matrix and an aqueous suspension of waxy maize starch nanocrystals as the reinforcing phase. It was shown that above 10 wt % starch nanocrystals form a continuous network within the NR matrix supposed to be held through hydrogen-bonding forces between nanoparticles. The existence of this network results in decreasing and increasing the diffusivity of toluene and water in composites, respectively. Furthermore, the morphological nature of starch nanocrystals confers to the materials barrier properties to water vapor and oxygen.[13]

To broaden the number of possible polymeric matrices by allowing the processing of composite materials from an organic solvent instead of aqueous suspensions and to achieve maximum interaction and adhesion between the filler and the matrix, the surface chemical modification of starch nanocrystals has been investigated.[14] Contact angle measurements have shown that the surface chemical modification of waxy maize starch nanocrystals with isocyanate and anhydride functions allowed enhancing the nonpolar nature of original starch nanocrystals.[14] Compared to unmodified nanoparticle-based composites, the resulting decrease of particle−particle H-bond interactions induced an increase of the toluene uptake and a decrease of the water uptake of NR/modified starch nanocrystals composite films.[13]

In the present paper, the mechanical properties of NR filled with starch nanocrystals were investigated through dynamic mechanical analysis, tensile tests, and successive tensile tests. Since starch nanocrystals are hydrophilic particles, the influence of humidity on mechanical properties was also investigated. The characterization of nanocomposite materials process from chemically modified nanoparticles was also performed.

Experimental Section

Materials. The materials used in the present study, i.e., starch nanocrystals and natural rubber (NR) latex, and the nanocomposite film processing have been described in our previous paper.[13] Waxy maize starch nanocrystals were prepared by H_2SO_4 hydrolysis of native waxy maize starch granules (Waxylis, Roquette S.A., Lestrem, France) according to a method described and optimized elsewhere.[11] They consist of platelet-like nanoparticles with a thickness of 6−8 nm, a length of 40−60 nm, and a width of 15−30 nm. The surface chemical modification of starch nanocrystals with alkenyl succinic anhydride (ASA) and phenyl isocyanate (PI) was

[†] CERMAV-CNRS.
[‡] EFPG-INPG.
* Corresponding author: e-mail Alain.Dufresne@efpg.inpg.fr.

10.1021/ma0512399 CCC: $30.25
Published on Web 10/01/2005

Table 1. Codification of the Samples

sample	filler	medium	starch content (wt %)	starch content (vol %)[a]
L100		water	0	0
LT100		toluene	0	0
L98	unmodified	water	2	1.29
L95			5	3.28
L90			10	6.69
L85			15	10.2
L80			20	13.9
L75			25	17.7
L70			30	21.7
ASA5	ASA-modified	toluene	5[b]	3.28[b]
ASA10			10[b]	6.69[b]
ASA20			20[b]	13.9[b]
ASA30			30[b]	21.7[b]
PI5	PI-modified	toluene	5[b]	3.28[b]
PI10			10[b]	6.69[b]
PI20			20[b]	13.9[b]
PI30			30[b]	21.7[b]

[a] Assuming densities of starch nanocrystals and NR as 1.55 and 1 g cm^{-3}, respectively. [b] In chemically modified filler based composites, it is worth noting the effect of the substituents on the volume and weight, i.e., density of the modified nanocrystals. At the same wt %, a composite with modified nanocrystals contains fewer crystals than a composite with unmodified nanocrystals as the modified nanocrystals should be heavier.

carried out using freeze-dried nanocrystals, and details were given in a previous paper.[14] NR was kindly supplied as latex by the Technical Center, MAPA (Liancourt, France). It contained spherical particles with an average diameter around 1 μm. The density of dry NR was 1 g cm^{-3}. The details for processing the NR/starch nanocrystals films from latex of NR and aqueous suspension of starch nanocrystals as well as the processing of composites filled with modified starch nanocrystals were given in a previous paper.[13] Films were conditioned at 0% relative humidity (RH) by storing in a desiccator containing P_2O_5 until being used. The codification of the samples is given in Table 1.

Dynamic Mechanical Analysis. Dynamic mechanical tests were carried out using a Rheometrics RSA2 spectrometer working in the tensile mode. Test conditions were chosen in such a way that the measurements obey the laws of linear viscoelasticity (the strain equaled 5×10^{-4}). The specimen was a thin rectangular strip ($30 \times 6 \times 0.8$ mm^3). The setup measured the complex tensile modulus E^*, i.e., the storage component E' and the loss component E''. The ratio between the two components, $\tan \delta = E''/E'$, was also determined. In the present work, results are displayed through E' and $\tan \delta$. Measurements were performed at 1 Hz, and the temperature was varied by steps of 3 K between 180 and 450 K.

Tensile Tests. The nonlinear mechanical behavior of starch nanocrystals filled composites was analyzed using an Instron 4301 testing machine working in tensile mode. Dumbbell-shaped specimens 4 mm wide, 7 mm long (L_0), and about 1 mm thick were used. The initial gap between pneumatic jaws was adjusted to 10 mm. Force (F)−elongation (e) curves were obtained for each sample at room temperature and with a cross-head speed of 10 mm min^{-1} (initial strain rate $d\epsilon/dt = 2.4 \times 10^{-2}$ s^{-1}).

The nominal strain (ϵ_{nom}) and the nominal stress (σ_{nom}) were calculated by $\epsilon_{nom} = e/L_0$ and $\sigma_{nom} = F/S_0$, respectively, where S_0 is the initial cross section. The true strain (ϵ_{true}) can be determined by $\epsilon_{true} = \ln(L/L_0)$, where L is the length of the sample during the test ($L = L_0 + e$). The true stress (σ_{true}) can be calculated by $\sigma_{true} = F/S$, where S is the cross section. S was determined assuming that the total volume of the sample remained constant during the test, so that $S = S_0L_0/L$. This assumption is strictly valid for the unfilled NR matrix at room temperature. Stress vs strain curves were plotted, and the Young's modulus (E) was measured from the slope of the low strain region. The conventional modulus $E_{100\%}$ was obtained from the slope of the straight line plotted between the origin $\sigma = \epsilon = 0$ and the point corresponding to a true strain of 100%.

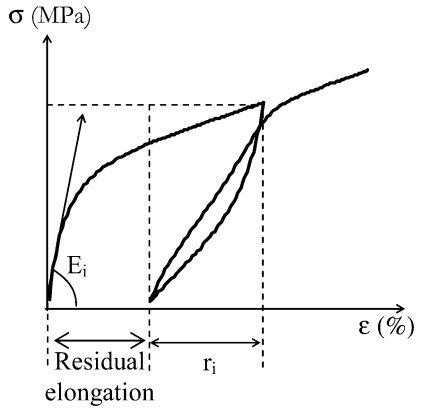

Figure 1. Schematic representation of the mechanical properties obtained for each cycle during successive tensile tests.

Ultimate mechanical properties were also characterized. The stress at break (σ_b) and the elongation at break (ϵ_b) were reported for each sample. Mechanical tensile data were averaged over at least five specimens.

Successive Tensile Tests. Successive tensile tests were performed to characterize the damage process occurring during tensile tests. They were carried out with the Instron 4301 machine under the same conditions as previously described. At the beginning of each experiment, the sample was first stretched under a load of 1.5 N. Then, the experiment consisted in stretching the sample up to a given elongation $\Delta L_1 = 10$ mm (cycle 1), then releasing the force down to 1.5 N, and stretching again the material up to $\Delta L_2 = 2\Delta L_1$ (cycle 2). This procedure was repeated with increasing elongation $\Delta L_i = i\Delta L_1$ until break of the sample. The tensile modulus E_i and the shrinkage r_i were determined for each successive cycle (Figure 1).

Results and Discussion

Dynamic Mechanical Analysis. a. Influence of Starch Content. Dynamic mechanical measurements were performed for NR films filled with different starch contents. The plot of the logarithm of the storage modulus, $\log(E')$, and the tangent of the loss angle, $\tan \delta$, vs temperature at 1 Hz are displayed in Figure 2.

The curve of $\log(E')$ corresponding to the unfilled matrix is typical of a fully amorphous high molecular weight thermoplastic behavior. For temperatures below the glass transition temperature, NR is in the glassy state: the storage modulus slightly decreases with temperature but remains roughly constant above 1 GPa. Then, a sharp decrease over 3 decades is observed around −60 °C, corresponding to the primary relaxation process associated with the glass−rubber transition determined by differential scanning calorimetry (DSC) measurements.[13] This modulus drop corresponds to an energy dissipation phenomenon displayed in the concomitant relaxation process where $\tan \delta$ passes through a maximum. Then, the modulus reaches a plateau around 1 MPa, corresponding to the rubbery state. The broad temperature range from −40 to 180 °C of the rubbery state is ascribed to the high molecular weight of the polymer, resulting in a highly entangled state of the macromolecules. Finally, around 190 °C the modulus decreases more rapidly, and the experimental setup fails to measure it. It corresponds to the irreversible flow of the material linked with the disentanglement of polymeric chains.

Starch nanocrystals have a significant reinforcing effect at temperatures higher than T_g. For instance, the relaxed modulus at room temperature (25 °C) of nano-

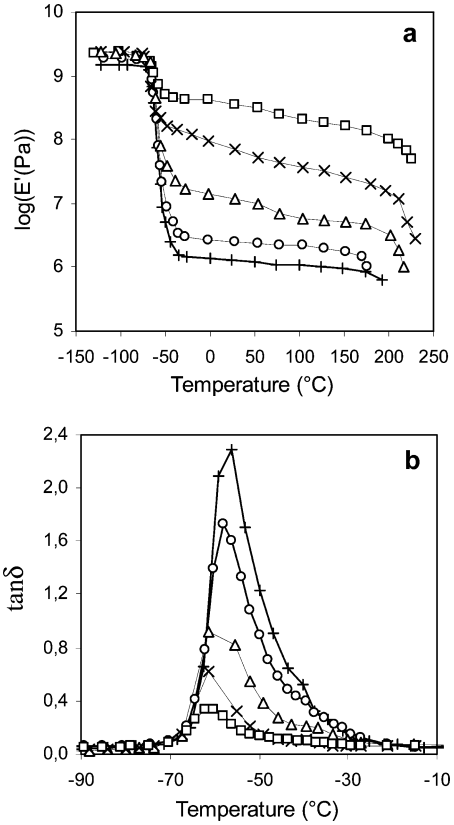

Figure 2. (a) Logarithm of the storage tensile modulus E' and (b) tangent of the loss angle tan δ vs temperature at 1 Hz for waxy maize starch nanocrystals/NR nanocomposite films: L100 (+), L95 (○), L90 (△), L80 (×), and L70 (□).

Table 2. Rubbery Storage Tensile Modulus Estimated at 25 °C (E'_{R25}) and Temperature Position (T_α) and Magnitude (I_α) of the tan δ Peak Associated with the α Relaxation Process for Waxy Maize Starch Nanocrystals/NR Nanocomposite Films

sample	E'_{R25} (MPa)	T_α (°C)	I_α
L100	1.28	−56	2.28
L95	2.48	−58	1.73
L90	12.3	−58	1.10
L80	96.0	−61	0.62
L70	257	−61	0.34

composite films containing 10, 20, and 30 wt % of filler is about 10, 75, and 200 times higher, respectively, than the one of the unfilled matrix (Table 2).

No significant improvement of the thermal stability of composites was induced when adding starch nanocrystals within the NR matrix. Actually, the matrix displays a rather high thermal stability, and starch begins to degrade at about the same temperature at which NR starts to totally disentangle and flow.

The evolution of tan δ with temperature displays a peak located in the temperature range of the glass transition of the NR matrix.[13] This relaxation process, labeled α, is associated with the anelastic manifestation of the glass−rubber transition of the polymer. This mechanism involves cooperative motions of long chain sequences. The temperature position (T_α) and magnitude of the peak (I_α) are listed in Table 2 for each composition. T_α and I_α decrease when adding starch nanocrystals. The decrease in T_α becomes significant for the 20 wt % starch reinforced material for which T_α decrease from −56 °C for the unfilled NR down to −61 °C. This is attributed to (i) the broadening of the glass−rubber transition zone toward lower temperatures reported from DSC measurements[13] and (ii) a classical mechanical coupling effect. (The shift of the tan δ peak results from the strong decrease of the modulus drop upon filler addition.) The reduction of the magnitude of I_α when increasing the starch nanocrystals content results from (i) the decrease of the number of mobile units participating to the relaxation process and (ii) the decrease of the magnitude of the modulus drop associated with T_g.

In a previous study,[15] the mechanical behavior of nanocomposite materials based on starch nanoparticles obtained from hydrochloric acid hydrolysis of potato starch granules and poly(styrene-*co*-butyl acrylate) [poly(S-*co*-BuA)] was investigated. It was concluded that the prediction of the modulus values by the modified Kerner equation developed for composites filled with particles of nearly spherical shape failed to describe the experimental values. In this approach, the composite modulus, E_c, is given by[16,17]

$$\frac{E_c}{E_m} = \frac{1 + ABv_f}{1 - B\psi v_f} \tag{1}$$

where E_m corresponds to the modulus of the unfilled matrix and v_f to the volume fraction of the filler. The constant A accounts for factors such as the geometry of the filler and the Poisson's ratio of the matrix and is therefore strongly dependent on the morphology of the material. It is related to the generalized Einstein coefficient k_E ($k_E = 2.5$ for unassociated spherical particles) by

$$A = k_E - 1 \tag{2}$$

The constant B takes into account the relative moduli of the filler and matrix phases. Its value is near 1.0 for fillers much more rigid than the polymer matrix. The factor ψ is a reduced concentration term related to the maximum packing fraction v_m of the filler. It is generally given by the following equation which fulfils the necessary boundary conditions:

$$\psi = 1 + \left(\frac{1 - v_m}{v_m^2}\right)v_f \tag{3}$$

The formation of aggregates or clustering of fillers within the thermoplastic matrix was accounted for in an ensuing paper[18] by varying the k_E value, which is known to increase with the number of spheres per aggregate. When fitting the data, two values for k_E were obtained, namely 70 and 400 for the low (v_f < 20 vol %) and high volume fraction (v_f > 20 vol %) regions, respectively. The intermediate composition (20 vol %) was found to correspond to an inflection point in the plot of the relaxed modulus and to a slope change in the plot of the water diffusion coefficient vs starch content. It was related to the existence of a percolating nanoparticles network within the sample above this value.

In our previous article,[13] it was also suspected from swelling experiments that a percolating starch nanocrystals network within the NR matrix may form, resulting from hydrogen-bonding forces between starch aggregates. This phenomenon, induced during the evaporation step of the material processing, should most probably affect the mechanical properties of the com-

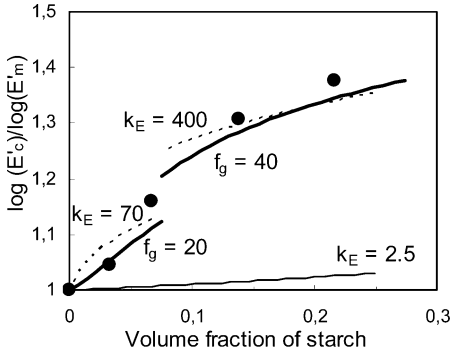

Figure 3. Ratio between the logarithm of the relaxed storage modulus estimated from DMA experiments at 25 °C of the composite film (E'_c) and the one of the matrix (E'_m) vs starch nanocrystals content. Filled circles represent the experimental data; solid line and dashed lines represent the calculated moduli using the generalized Kerner prediction (eq 1) with $k_E = 2.5$ and $k_E = 70$ (low volume fractions region) or $k_E = 400$ (high volume fractions region), respectively. Bold solid lines represent the calculated moduli using the Guth prediction modified for nonspherical particles (eq 4) with $f_g = 20$ (low volume fractions region) and $f_g = 40$ (high volume fractions region).

posites in the linear range. In swelling experiments, changing behavior was reported above 10 wt % (around 6.7 vol %) of starch nanocrystals.[13] In the percolation approach, the percolation threshold is found to depend for one thing on the aspect ratio of the percolating species. Here, this value cannot be easily defined since the connecting particles should be starch clusters or aggregates with ill-defined size and geometry.

Figure 3 shows the evolution of the ratio of the logarithm of the relaxed storage modulus at room temperature (25 °C) of waxy maize starch nanocrystals reinforced NR films and unfilled matrix vs nanoparticles content. The continuous line corresponds to the evolution of the predicted modulus using the generalized Kerner equation (eq 1) with $k_E = 2.5$. Calculation was performed taking $v_m = 0.6$, corresponding to a body-centered-cubic arrangement of spherical particles. Obviously, these calculated data disagree with the experimental ones. The dashed lines correspond to the predicted modulus assuming the same k_E values than those reported for potato starch nanocrystals reinforced poly(S-*co*-BuA). However, the discontinuity in predicted data was set at 6.7 vol %, i.e., 10 wt %, instead of 20 vol %. Surprisingly, a rather good agreement is observed between predicted and experimental data despite the different natures of the filler, the acid used for the preparation of the nanocrystals, and the matrix. This is an indication that the morphology of the highly irregular aggregates is similar for both systems. However, the concentration for which the nanoparticle clusters start to aggregate is about 3 times lower for nanocrystals obtained from waxy maize starch and prepared using sulfuric acid. Additional experimental data and intermediate compositions are necessary to fully confirm this finding.

For potato starch nanocrystals reinforced poly(S-*co*-BuA), modulus values were also predicted[18] by the Guth equation,[19] modified for nonspherical particles:[20]

$$E_c = E_m(1 + 0.67 f_g v_f + 1.62 f_g^2 v_f^2) \qquad (4)$$

where f_g is the sphericity coefficient or shape factor, which is defined as the ratio of particle length to width.

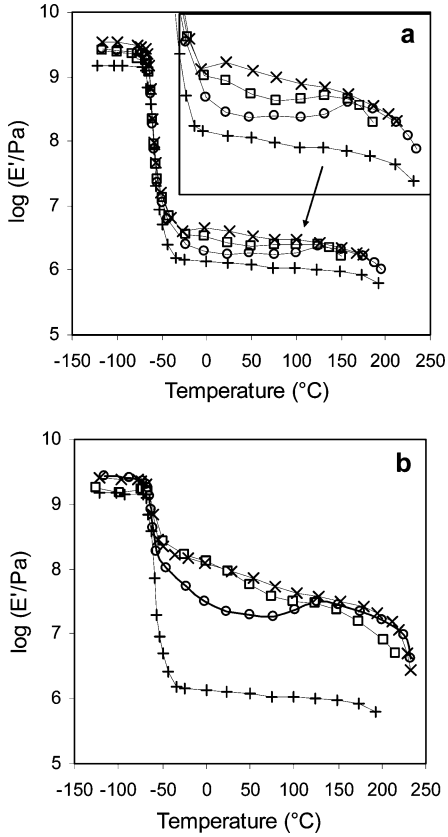

Figure 4. Logarithm of the storage tensile modulus E' vs temperature for waxy maize starch nanocrystals/NR nanocomposite films: L100 (+), (a) L95 and (b) L80 conditioned at 0 (×), 43 (□), and 98% RH (○).

In the previous study,[18] the f_g value was used as an adjustable parameter in the attempt to fit the experimental data with the Guth model. Two values for f_g were obtained, namely 20 and 40 for the low ($v_f < 20$ vol %) and high volume fraction ($v_f > 20$ vol %) regions, respectively. These values were applied to fit the experimental data of the relaxed tensile storage modulus observed at room temperature (25 °C) for waxy maize starch nanocrystals reinforced NR (Figure 3, bold lines). Again, a rather good agreement between predicted and experimental data is reported.

b. Influence of Moisture Content. To study the effect of moisture content, 5 and 20 wt % filled materials were stored in different relative humidity (RH) conditions, viz. 0, 43, and 98% RH. The saturated salt solutions were P_2O_5, $K_2CO_3 \cdot 3H_2O$, and $CuSO_4 \cdot 5H_2O$, respectively. Figure 4 shows the effect of storage RH conditions on the evolution of the logarithm of the storage modulus vs temperature for 5 and 20 wt % filled materials. The curve corresponding to the unfilled NR matrix has been added as reference. The behavior of both composite compositions is affected by the water content. The higher the water content is, the lower the rubbery modulus is. Water uptake experiments showed that the hydrophilic filler was mainly responsible of the water sensitivity of the studied composites.[13] The diminution of the reinforcing capability of starch nanoparticles should be ascribed to the possible formation of a soft water-rich filler/matrix interphase when storing the materials in moist conditions. This soft interphase could hinder the stress transfer at the interface when submitting the material to a mechanical solicitation. However, regardless the moisture condition the relaxed modulus

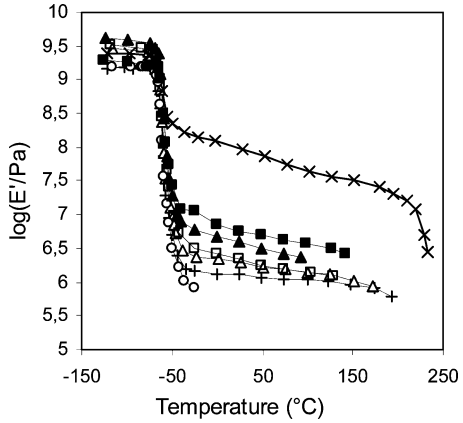

Figure 5. Logarithm of the storage tensile modulus E' vs temperature at 1 Hz for waxy maize starch nanocrystals/NR nanocomposite films: L100 (+), L80 (×), LT100 (○), ASA20 (□), ASA30 (■), PI20 (△), and PI30 (▲).

of composites remained higher than the one of the unfilled NR matrix. No shift of the temperature corresponding to the modulus drop associated with T_g and resulting from a plasticization effect of water on NR was reported as well. Around 100 °C, the rubbery modulus of wet samples, i.e., materials stored at 43 or 98% RH, increases until reaching the same modulus value than the one obtained for the material stored at 0% RH. In this range of temperatures, a progressive dehydration of the material occurred, and the curves corresponding to the different water contents tended to merge.

c. Effect of Chemical Modification. Figure 5 shows the evolution of the logarithm of the storage modulus vs temperature for unfilled matrices processed by either water evaporation of the latex (L100) or toluene evaporation of solubilized NR in toluene (LT100). No difference in the temperature range of the modulus drop associated with T_g was reported. However, it was observed that the setup failed to measure the relaxed storage modulus of LT100 because the flow of the material occurred very rapidly beyond the modulus drop associated with T_g. This should be ascribed to the only difference between the two unfilled matrices, that is, the solubilization step and the necessary vigorous stirring of the solution. During this procedure, the polymer chains could be mechanically degraded and broken.

No reinforcing effect was observed for composite materials filled with 5 and 10 wt % of chemically modified starch nanocrystals using either ASA or PI (not shown in Figure 5). For composite materials filled with 20 wt % of modified nanocrystals, the reinforcing effect in the rubbery state of the NR matrix was found to be much lower than the one reported for unmodified starch nanoparticles filled systems. Even when the chemically modified starch nanocrystals content was 30 wt %, the relaxed modulus remained much lower than the one of the 20 wt % unmodified particles filled NR. The thermal stability was also strongly reduced upon surface chemical modification of the filler. Despite the different mechanical behavior of the unfilled matrices when using either unmodified or chemically modified starch nanoparticles, this is an indication of an unusual behavior. Contrarily to classical composite science in which improvement of the interfacial adhesion usually results in improved properties, the compatibilization of the starch nanofiller induces a dramatic decrease of the performance of the material. This could be ascribed to

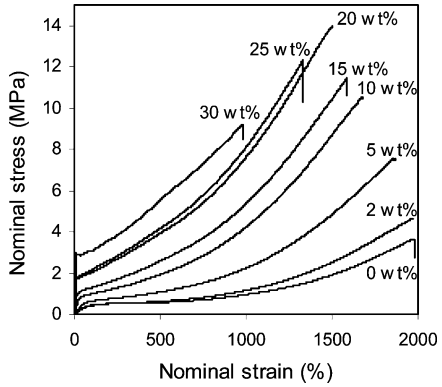

Figure 6. Typical nominal stress vs nominal strain curves of waxy maize starch nanocrystals/NR nanocomposite films. The starch nanocrystals contents are indicated in the figure.

the original reinforcing effect of starch nanocrystals through the formation of a hydrogen-bonded percolating filler network above a given starch content. Coating of the filler should result in a decrease of the possible H bonds between adjacent particles or aggregates of particles. Similar observations were reported for chitin whiskers reinforced NR.[21] In our previous study,[13] it was found that the surface chemical modification of starch nanocrystals resulted in a favored swelling behavior with toluene, ascribed to lower interactions between filler particles. However, the positive aspect of the use of chemically modified starch nanocrystals is that the cohesion and the thermal stability of the rubbery matrix obtained from toluene evaporation of solubilized NR in toluene (LT100) are strongly increased upon filler addition.

A clear tendency is also observed depending on the nature of the chemical coupling agent. For a given composition, the ASA-treated samples display a systematically higher rubbery modulus than their isocyanate counterparts. This was also already observed for chitin whiskers.[21] This result is in agreement with the swelling behavior of the materials, which was studied elsewhere.[13] It was shown that the toluene uptake was higher for isocyanate-modified starch nanoparticles filled than for ASA-modified filler-based composites. This was ascribed to comparatively stronger interactions between ASA-modified filler and the matrix. The increase of the filler/matrix interactions results in a decrease of filler/filler interactions which are responsible for high mechanical properties.

Tensile Tests. a. Influence of Starch Content. The tensile mechanical properties of the NR/starch nanocrystals composites were studied at room temperature. Typical curves of stress vs strain (nominal data) are plotted in Figure 6. The samples exhibit an elastic nonlinear behavior typical of amorphous polymers at $T > T_g$. The stress regularly increases with the strain up to the break of the film.

The evolution of the nominal elongation at break, nominal stress at break, and tensile modulus is plotted in Figure 7 as a function of the starch content. Figure 7 also displays the evolution of the nominal stress at break vs elongation at break. Data are collected in Table 3.

As expected, the elongation at break decreases with increasing starch content (Figure 7a). This diminution in elastic properties is not linear. Up to a starch nanocrystals content around 20 wt %, ϵ_b slightly decreases from 1960 to 1500% and then decreases more

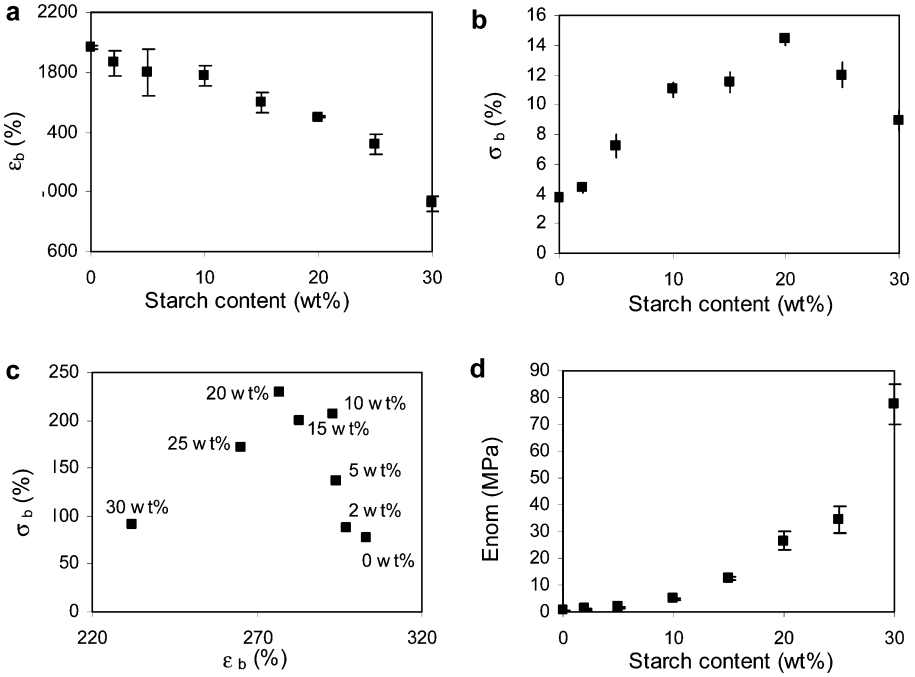

Figure 7. Nominal (a) elongation at break, (b) strength, and (d) tensile modulus for waxy maize starch nanocrystals/NR nanocomposite films vs starch content. (c) Nominal strength vs nominal elongation at break (the starch nanocrystals contents are indicated in panel c).

Table 3. Mechanical Properties of Waxy Maize Starch Nanocrystals/NR Nanocomposite Films Obtained from Tensile Tests: Nominal and True Tensile Modulus (*E*), Strength (σ_b), and Elongation at Break (ϵ_b)

	E (MPa)			σ_b (MPa)		ϵ_b (%)	
sample	nominal	true	$E_{100\%}$[a]	nominal	true	nominal	true
L100	0.65	0.87	0.4	3.7	77.1	1963	303
L98	1	1.4	0.46	4.4	87.1	1859	297
L95	1.6	2.2	0.64	7.2	136.8	1796	294
L90	4.9	6.1	1	11	205.6	1773	293
L85	12.5	14.4	1.3	11.5	199.3	1597	283
L80	26.5	29.7	2	14.4	229.5	1500	277
L75	34.3	37.9	2.2	12	170.5	1312	265
L70	77.8	85.8	3.2	8.9	90.9	920	232

[a] $E_{100\%}$ corresponds to the conventional tensile modulus at 100% elongation.

rapidly down to 920% for the NR film filled with 30 wt % starch nanoplatelets. The nominal stress at break passes through a maximum for a weight fraction of 20 wt % (Figure 7b). The decrease of σ_b for starch content higher than 20 wt % is linked with the sharp decrease in ϵ_b values. The increasing brittleness of the composite material induces a decrease of its strength. Considering the ultimate properties, a good compromise between the increase of the strength and the decrease of the elongation at break seems to be reached for a starch content around 20 wt % (Figure 7c). The tensile modulus increases nearly exponentially with starch content (Figure 7d), from 0.64 MPa for the unfilled NR matrix up to 77.8 MPa for composite films filled with 30 wt %. These values are lower than the storage tensile modulus values reported from DMA experiments at room temperature (Table 2). However, it is worth noting that in DMA analysis the adhesion between the filler and the matrix is less involved than in tensile tests because of weaker stresses applied in the former technique. This result is therefore an indication of the lack of intimate adhesion between both components of the composite structure.

The reinforcing effect of starch nanocrystals was compared to the one of other fillers for NR published in the literature such as clays, organoclays, carbon black, flyash, and chitin whiskers. The relative values of the conventional tensile modulus at 100% elongation, strength, and elongation at break, which correspond to the ratio of a given property divided by the one of the unfilled NR matrix, are collected in Table 4. Except for films reinforced with chitin whiskers, the NR matrix is systematically cross-linked (labeled CNR in Table 4) whereas it is unvulcanized for our data. This difference can have an importance mainly for ultimate properties. Starch nanocrystals present better mechanical properties than flyash.[22] They are clearly a good substitute for carbon black since the addition of only 10 wt % of starch nanoparticles to NR induces a reinforcing effect similar, in terms of stiffness, to the one observed with 26.6 wt % carbon black.[3] In addition, high starch nanocrystals contents seem to preserve the elastic behavior of NR-based composites, contrarily to carbon black. Indeed, the decrease of the elongation at break is more progressive for the starchy filler than for carbon black, which induces a high brittleness of the material with only a few percent. However, starch nanocrystals are not as competitive as organoclays.[3] This could be ascribed to the higher aspect ratio of exfoliated organoclay nanoplatelets. Compared to chitin whiskers, starch nanocrystal-based nanocomposites display a lower tensile modulus but higher ultimate properties (both higher strength and elongation at break) for 5 wt % filler content.[23] This is due to the higher aspect ratio and completely different geometry of rodlike chitin nanocrystals and thus a lower percolation threshold.

b. Influence of Evaporation Temperature. As described in the Experimental Section, a temperature of 40 °C was chosen for the evaporation step during composite processing. For this choice, we were faced to several problems. On one hand, we wish reducing the duration of film processing and, at the same time, limiting the possible sedimentation of starch nanocrys-

Table 4. Comparison of Relative Mechanical Properties of NR Filled with Different Types and Contents of Filler: Relative Conventional Tensile Modulus at 100% Elongation ($E_{R100\%}$), Relative Strength (σ_{Rb}), and Relative Elongation at Break (σ_{Rb})

sample	$E_{R100\%}$	σ_{Rb}	ϵ_{Rb}	ref
NR-5 wt % of starch nanocrystals	1.6	1.95	0.91	our study
NR-10 wt % of starch nanocrystals	2.5	2.97	0.9	our study
NR-20 wt % of starch nanocrystals	5	3.89	0.76	our study
CNR-14.2vol % of flyash	0.97	2.68	~1	22
CNR-8.3 wt % of carbon black	1.41	1.16	0.66	3
CNR-26.6 wt % of carbon black	2.71	2.42	0.62	3
CNR-8.3 wt % of unmodified clay	0.90	0.85	0.79	3
CNR-8.3 wt % of organoclay	2.92	3.53	~1	3
NR-5 wt % of chitin whiskers	2.78	1.76	0.53	23

Table 5. Mechanical Properties of Waxy Maize Starch Nanocrystals Filled NR Nanocomposites Obtained from Tensile Tests: Tensile Modulus (E), Nominal Strength (σ_b), and Nominal Elongation at Break (ϵ_b)[a]

sample	T (°C)	ϵ_b (%)	σ_b (MPa)	E (MPa)
L90	40	1773	11	4.9
	60	1547	6	6.2
	70	1424	4.2	3.9
	80	1439	4.1	3.2
sample	RH (%)	ϵ_b (%)	σ_b (MPa)	E (MPa)
L80	0	1500	14.4	26.5
	35	1491	11.5	17
	43	1490	11.4	14.8
	58	1466	7.2	12.5
	75	1406	6.1	9.7
	98	1443	2.7	5.7

[a] Films were processed at different temperatures (T) for film L90 or conditioned at different RH conditions for film L80.

Table 6. Mechanical Properties of Modified Waxy Maize Starch Nanocrystal Filled NR Nanocomposites Obtained from Tensile Tests: Tensile Modulus (E), Nominal Strength (σ_b), and Nominal Elongation at Break (ϵ_b)

sample	ϵ_b (%)	σ_b (MPa)	E (MPa)
LT100	1550	0.53	0.42
ASA5	1457	0.59	0.54
ASA10	1502	0.65	0.56
ASA20	1680	1.1	0.83
PI5	1216	0.4	0.47
PI10	897	0.56	0.7
PI20	956	0.65	0.86

tals in NR latex. For this, films should be evaporated at temperatures higher than room temperature. On the other hand, it is well-known that starch gelatinization occurs in excess of water around 80 °C. Gelatinization corresponds to an irreversible swelling followed by a solubilization of starch particles, resulting in the loss of its crystalline structure. Thereby, we have chosen to evaporate the NR/starch nanocrystals mixtures at different temperatures ranging from 40 to 80 °C and to study the influence of this temperature on tensile properties of composite films. Tensile tests were performed on films filled with 10 wt % of starch, obtained by evaporation at 40, 60, 70, and 80 °C.

When increasing the evaporation temperature, it was found that all the tensile properties decreased (Table 5). The diminution of both tensile modulus and strength was assumed to be due to a decrease of the actual content of crystalline filler ascribed to their loss of crystallinity and therefore of their reinforcing capability. Above 70 °C the tensile properties did not change any more and results obtained for films obtained by water evaporation at 70 and 80 °C are similar. In addition, a low evaporation temperature allows letting time for the possible formation of a percolating network of starch nanocrystals held through hydrogen bonds. Furthermore, it allows having a homogeneous drying, thereby avoiding the formation of a crust at the surface of the film. Additional tests were performed for 5 wt % filled materials and corroborated these results (data not shown). According to these results, the evaporation at room temperature would most probably favor the reinforcing effect of starch nanocrystals, but also slow down the film processing duration. No experiment has been performed to check this assumption. This study justifies the choice of 40 °C for the evaporation temperature.

c. Influence of Moisture Content. NR-based nanocomposite materials filled with 5 and 20 wt % starch nanocrystals were stored in different relative humidity conditions, namely 0, 35, 43, 58, 75, and 98% RH. The respective saturated salt solutions were P_2O_5, $CaCl_2 \cdot 6H_2O$, $K_2CO_3 \cdot 3H_2O$, $NaBr \cdot 2H_2O$, NaCl, and $CuSO_4 \cdot 5H_2O$. The tensile properties obtained for L80 films are given in Table 5. The relative humidity does not affect significantly the elongation at break which remained between 1400 and 1500%. However, when increasing the RH conditions, the strength decreased from 14.4 MPa for the film stored at 0% RH down to 2.7 MPa for the film stored at 98% RH. Similarly, the tensile modulus decreased from 26.5 MPa (0% RH) down to 5.7 MPa (98% RH), in agreement with DMA measurements performed on composite materials stored in different humidity conditions. Similar observations were reported for sample L95.

d. Effect of Chemical Modification. The tensile nonlinear mechanical properties of modified starch nanocrystals/NR composite films are collected in Table 6. The evolution of the relative tensile modulus and ultimate properties vs starch content is shown in Figure 8. Data corresponding to the NR filled with unmodified nanoparticles are added as reference (filled circles). Plotting relative mechanical data allows comparing the performances of unmodified and chemically modified nanoparticle-based composites despite the different properties of the matrix obtained from an aqueous or toluene mixture. Comparing first the mechanical properties of unfilled matrices L100 (Table 3) and LT100 (Table 6), it appears that no significant differences are reported for the modulus value. However, both the strength and the elongation at break are much higher for the film processed from an aqueous suspension. This is mainly ascribed to the higher molecular weight of this polymer compared to the toluene dissolved one, in agreement with DMA experiments. The ultimate properties are very sensitive to the number of entanglements per chain. As reported from DMA tests, the reinforcing effect of starch nanocrystals displayed through the tensile modulus is much lower for modified nanoparticles than for unmodified ones (panel a). This is

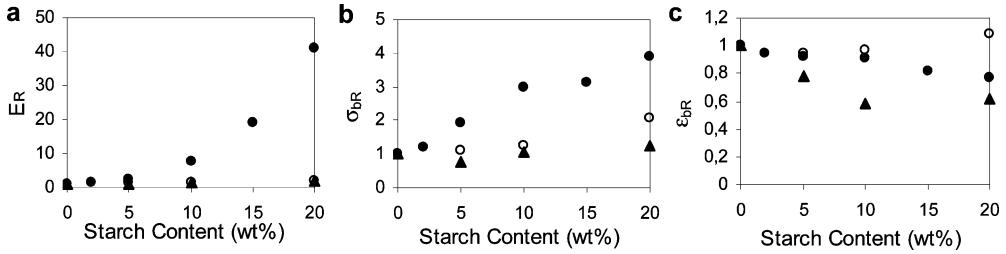

Figure 8. Relative (a) tensile modulus E_R, (b) strength σ_{bR}, and (c) elongation at break ϵ_{bR} for waxy maize starch nanocrystals/NR nanocomposite films: unmodified (●), ASA-modified (○), and PI-modified (▲) nanoparticles.

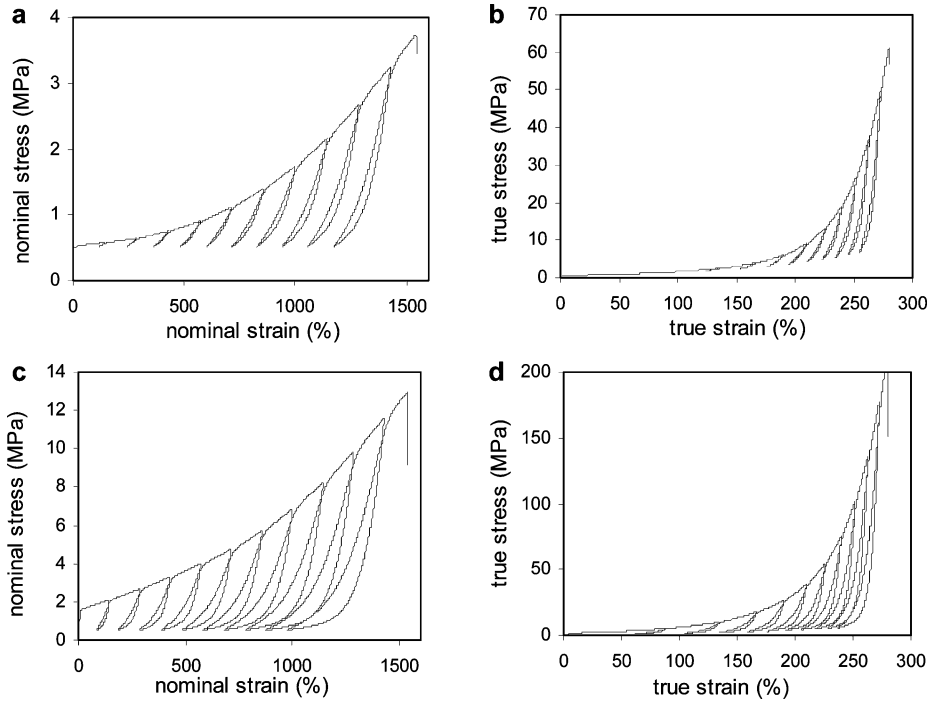

Figure 9. Evolution of (a, c) the nominal stress vs nominal strain and (b, d) the true stress vs true strain for waxy maize starch nanocrystals/NR nanocomposite films during successive tensile tests: L100 (panels a and b) and L80 (panels c and d).

ascribed to hindered interactions between chemically modified particles resulting from their coating with the grafting agent. However, weak differences were observed between ASA- and PI-modified fillers. As expected and consequently, the ultimate tensile strength of modified starch nanocrystal-based composites is systematically lower than for unmodified filler-based materials (panel b). However, composite materials processed using ASA-modified particles displayed higher strengths than films reinforced with PI-modified particles. The evolution of the relative elongation at break is more difficult to explain since it results from two opposite effects. On one hand, the increased filler/matrix interfacial adhesion and decreased strength reported for modified particle-based composites should result in a decrease of ϵ_b. On the other hand, the decreased particle−particle interactions should result in an increase of ϵ_b. It seems that the former phenomenon is preponderant for PI-modified particles whereas the latter mainly govern the behavior of ASA-modified particles filled composites.

Successive Tensile Tests. Successive tensile tests were performed for all waxy maize starch nanocrystals/NR films. Figure 9 shows the typical evolution of nominal stress vs nominal strain (panels a and c) and of true stress vs true strain (panels b and d) for the unfilled NR matrix L100 (panels a and b) and L80 films (panels c and d). We can observe that the curves obtained during the stretching step (positive elongation rate) and the ones obtained during the recovery step (negative elongation rate) are not superimposed. In addition, after each cycle, a residual elongation is induced. This is due to the entropic origin of the strain and to the participation of the viscoelastic component to the total compliance. However, it is worth noting that for a given temperature this effect is strongly time dependent and that its magnitude is mainly governed by the strain rate applied during the experiment. For latter cycles it is also possible that the material could be stretched up to elongations higher than its elastic limit because the rubber is unvulcanized.

The nominal tensile modulus E_i and the shrinkage r_i corresponding to the difference between the elongation ΔL_i and the residual elongation retained at the end of each cycle (Figure 1) were determined for each cycle and all compositions. Their evolution as a function of both the starch content and the number of successive cycles are plotted in the three-dimensional diagrams of Figure 10. For the sake of clarity, the modulus scale in Figure 10a was restricted to 8 MPa. The whole experimental data are collected in Table 7.

For the unfilled NR matrix, the tensile module continuously increases during successive cycles. This phenomenon is ascribed to the strain-induced crystallization of NR. Indeed, it was demonstrated that the birefringence and the crystallinity measured by X-ray

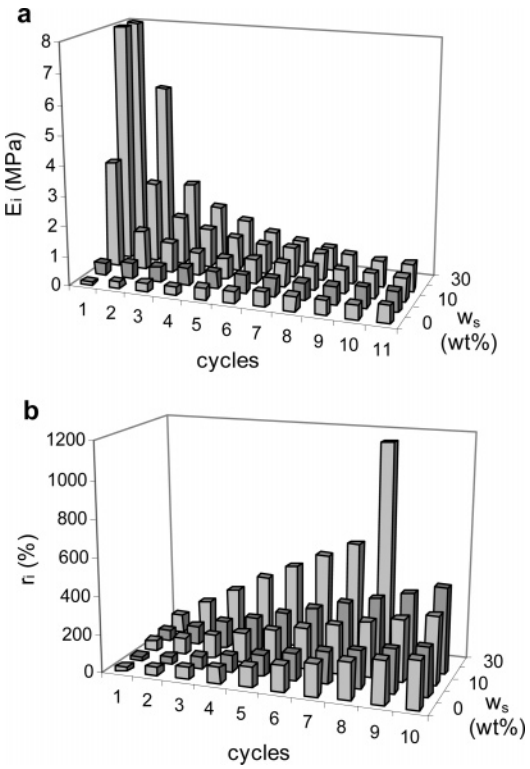

Figure 10. Evolution of (a) the nominal tensile modulus E_i and (b) the shrinkage r_i measured for cycle i for waxy maize starch nanocrystals/NR nanocomposite films during successive tensile tests as a function of i and of the starch nanocrystals content w_s.

Table 7. Tensile Modulus E_i (MPa) and Shrinkage r_i (%) Determined for Waxy Maize Starch Nanocrystals/NR Nanocomposite Films during Successive Tensile Tests I

sample	E_1	E_2	E_3	E_4	E_5	E_6	E_7	E_8	E_9	E_{10}	E_{11}
L100	0.1	0.2	0.3	0.3	0.4	0.4	0.5	0.5	0.5	0.5	0.6
L98	0.2	0.3	0.3	0.3	0.4	0.4	0.4	0.5	0.5	0.5	0.5
L95	0.4	0.5	0.5	0.6	0.6	0.6	0.6	0.6	0.6	0.7	0.7
L90	3.6	1.3	1.0	0.8	0.7	0.8	0.8	0.8	0.8	0.8	0.8
L85	6.3	1.7	1.0	0.8	0.7	0.7	0.7	0.6	0.6	0.6	0.6
L80	25.9	2.7	1.6	1.3	1.1	1.0	1.0	0.9	1.0	0.9	0.9
L75	28.8	4.6	2.2	1.7	1.4	1.0	0.9	0.9	0.7	0.6	0.6
L70	59.7	5.8	2.5	1.8	1.4	1.1	0.9	0.8			

sample	r_1	r_2	r_3	r_4	r_5	r_6	r_7	r_8	r_9	r_{10}
L100	22	43	63	86	112	139	171	200	229	253
L98	38	62	81	102	124	150	181	211	241	269
L95	21	41	64	89	116	144	173	200	229	257
L90	53	90	123	156	190	225	258	291	325	361
L85	55	94	131	168	206	246	285	324	364	406
L80	59	103	145	186	231	274	321	364	409	456
L75	91	173	250	323	399	475	557	639	750	798
L70	97	187	274	359	440	517	594	1143		

diffraction of NR increased with strain.[24,25] It was concluded that strain-induced crystallization started for a strain around 400%.[26] The maximum achievable crystallinity was found to be around 30% by WAXS analysis[27] and around 20% by high-resolution solid-state ^{13}C NMR spectroscopy.[28] More recently, it was discovered that only a low fraction of the amorphous NR chains are oriented and subsequently crystallized during stretching, carrying most of the applied load.[29] In our case, the modulus increases from the second cycle, revealing that the crystallization begins before having reached a strain of 400%. Indeed, the initial length of the sample, $L_0 = 7$ mm, is of the same order of magnitude as the elongation at each cycle, $\Delta L_1 = 10$ mm. The strain at the beginning of the second cycle is therefore lower than 400%. Such a continuous modulus increase during successive tensile tests is observed for low starch contents composites (up to 5 wt %). This means that the behavior of the poorly filled nanocomposite films is mainly governed by the one of the matrix. It could be ascribed to the absence of a continuous nanocrystals network within the NR matrix.

For highly filled nanocomposite materials (starch content higher than 5 wt %) the tensile modulus decreases during the first five cycles. The higher the starch content is, the stronger the modulus drop is (Table 7). This modulus drop during the early successive tensile experiments could be ascribed to the progressive disruption of the continuous starch nanocrystals network. The higher the starch nanoparticles content is, the closer the continuous network is and the stronger the effect of the disruption is. Furthermore, it was already shown that the addition of filler (carbon black, for instance) decreases the capability of NR chains to crystallize.[29] After the fifth cycle, the modulus remains roughly constant. This should indicate that complete disruption of the continuous starch network was achieved and that no strain-induced crystallization of the film occurred at this stage. This is an indication that a nominal strain around 700% is necessary for the complete disruption of the percolating nanoparticles network. It was also observed that for a given cycle the modulus increases with the starch content (Table 7). This reinforcing effect agrees with both DMA and tensile tests results.

Regardless of the composition, the shrinkage increases for each additional successive tensile cycle. It is about 10 times higher for the tenth cycle than for the first one (Figure 10b and Table 7). These data suggest that viscous flow in the samples decreases at each cycle whereas the elastic recovery component increases. When increasing the starch nanoparticles content, the shrinkage becomes more important; i.e., the residual elongation decreases for a given cycle (Figure 10b). The presence of the filler induces a more elastic behavior of the material and decreases at the same time its viscoelasticity.

Conclusion

Waxy maize starch nanocrystals appeared to be an effective reinforcing agent for natural rubber at temperatures higher than the glass transition temperature of the matrix. The relaxed modulus at room temperature (25 °C) of nanocomposite films containing 10, 20, and 30 wt % of filler is about 10, 75, and 200 times higher, respectively, than the one of the unfilled matrix. It was shown that up to a content of 20 wt % this new filler presents the advantage to effectively reinforce NR without decreasing significantly the elongation at break of the material. All the results show that particle−particle interactions play a crucial role in the properties of starch nanocrystals filled NR. Any deterioration of these interactions results in a dramatic decrease of the mechanical performances of the ensuing composites.

The addition of only 10 wt % of starch nanoparticles to NR induces a reinforcing effect similar, in terms of stiffness, to the one observed with 26.6 wt % carbon black. Furthermore, high starch nanocrystals contents seem to preserve the elastic behavior of NR-based composites, contrarily to carbon black. In conclusion, even if starch nanocrystals are not so competitive than

organoclays, they are clearly a good substitute for carbon black.

Acknowledgment. The authors are grateful to Mrs. C. Crépeau (Technical Center, MAPA Co., Liancourt, France) and Mr. Serpeloni (Roquette Frères S.A., Lestrem, France) for the supply of NR latex and waxy maize starch, respectively.

References and Notes

(1) Nideröst, K. J.; Walters, M. H. In *Polymer Matrix Composites*; Taljera, R., Manson, J.-A. E., Eds.; Elsevier: Amsterdam, 2001; pp 77−105.
(2) Vu, Y. T.; Mark, J. E.; Pham, L. H.; Engelhardt, M. *J. Appl. Polym. Sci.* **2001**, *82*, 1391−1403.
(3) Arroyo, M.; Lopez-Manchado, M. A.; Herrero, B. *Polymer* **2003**, *44*, 2447−2453.
(4) Bala, P.; Samantaray, B. K.; Srivastava, S. K.; Nando, G. B. *J. Appl. Polym. Sci.* **2004**, *92*, 3583−3592.
(5) Nah, C.; Ryu, H. J.; Kim, W. D.; Choi, S. S. *Polym. Adv. Technol.* **2002**, *13*, 649−652.
(6) Varghese, S.; Karger-Kocsis, J. *Polymer* **2003**, *44*, 4921−4927.
(7) Nah, C.; Ryu, H. J.; Kim, W. D.; Chang, Y. W. *Polym. Int.* **2003**, *52*, 1359−1364.
(8) Kim, J. T.; Oh, T. S.; Lee, D. H. *Polym. Int.* **2003**, *53*, 406−411.
(9) Sadhu, S.; Bhowmick, A. K. *J. Appl. Polym. Sci.* **2004**, *92*, 698−709.
(10) Putaux, J. L.; Molina-Boisseau, S.; Momaur, T.; Dufresne, A. *Biomacromolecules* **2003**, *4*, 1198−1202.
(11) Angellier, H.; Choisnard, L.; Molina-Boisseau, S.; Ozil, P.; Dufresne, A. *Biomacromolecules* **2004**, *5*, 1545−1551.
(12) Angellier, H.; Putaux, J.-L.; Molina-Boisseau, S.; Dupeyre, D.; Dufresne, A. *Macromol. Symp.* **2005**, *221*, 95−104.
(13) Angellier, H.; Molina-Boisseau, S.; Dufresne, A. *Macromolecules* **2005**, *38*, 3783−3792.
(14) Angellier, H.; Molina-Boisseau, S.; Belgacem, M. N.; Dufresne, A. *Langmuir* **2005**, *21*, 2425−2433.
(15) Dufresne, A.; Cavaillé, J. Y.; Helbert, W. M*acromolecules* **1996**, *29*, 7624−7626.
(16) Lewis, T. B.; Nielsen, L. E. *J. Appl. Mater. Sci.* **1970**, *14*, 1449−1471.
(17) Nielsen, L. E. *J. Appl. Phys.* **1970**, *41*, 4626−4627.
(18) Dufresne, A.; Cavaillé, J. Y. *J. Polym. Sci., Part B: Polym. Phys.* **1998**, *36*, 2211−2224.
(19) Guth, E. *J. Appl. Phys.* **1945**, *16*, 20−25.
(20) Ahmed, S.; Jones, F. R. *J. Mater. Sci.* **1990**, *25*, 4933.
(21) Gopalan Nair, K. G.; Dufresne, A.; Gandini, A.; Belgacem, M. N. *Biomacromolecules* **2003**, *4*, 1835−1842.
(22) Hundiwale, D. G.; Kapadi, U. R.; Desai, M. C.; Bidkar, S. H. *J. Appl. Polym. Sci.* **2002**, *85*, 995−1001.
(23) Gopalan Nair, K.; Dufresne, A. *Biomacromolecules* **2003**, *4*, 666−674.
(24) Treloar, R. G. *Trans. Faraday Soc.* **1947**, *43*, 277 and 284.
(25) Shimomura, Y.; White, J. L.; Spruiell, J. E. *J. Appl. Polym. Sci.* **1982**, *27*, 3553−3567.
(26) Toki, S.; Fujimaki, F.; Okuyama, M. *Polymer* **2000**, *41*, 5423−5429.
(27) Mitchell, G. R. *Polymer* **1984**, *25*, 1562−1572.
(28) Lin, W.; Bian, M.; Yang, G.; Chen, Q. *Polymer* **2004**, *45*, 4939−4943.
(29) Toki, S.; Sics, I.; Ran, S.; Liu, L.; Hsiao, B. S. *Macromolecules* **2002**, *35*, 6578−6584.

MA0512399